ACS chemical biology

Letters

pubs.acs.org/acschemicalbiology

Ligand Optimization by Improving Shape Complementarity at a Hepatitis C Virus RNA Target

Brian P. Charrette,[†,§] Mark A. Boerneke,[†] and Thomas Hermann*[,†,‡]

[†]Department of Chemistry and Biochemistry, University of California, San Diego, 9500 Gilman Drive, La Jolla, California 92093, United States

[‡]Center for Drug Discovery Innovation, University of California, San Diego, 9500 Gilman Drive, La Jolla, California 92093, United States

Supporting Information

ABSTRACT: Crystal structure analysis revealed key interactions of a 2-amino-benzimidazole viral translation inhibitor that captures an elongated conformation of an RNA switch target in the internal ribosome entry site (IRES) of hepatitis C virus (HCV). Here, we have designed and synthesized quinazoline derivatives with improved shape complementarity at the ligand binding site of the viral RNA target. A spiro-cyclopropyl modification aimed at filling a pocket in the back of the RNA binding site led to a 5-fold increase of ligand affinity while a slightly more voluminous dimethyl substitution at the same position did not improve binding. We demonstrate that precise shape complementarity based solely on hydrophobic interactions contributes significantly to ligand binding even at a hydrophilic RNA target site such as the HCV IRES conformational switch.

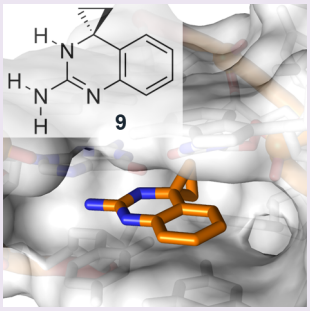

Viral RNA genomes and transcripts contain noncoding RNA (ncRNA) elements which may adopt complex three-dimensional folds and provide potential targets for the development of antiviral drugs.[1] Such structured ncRNA motifs have been recognized as key participants of many biological processes.[2] The well-defined structure of RNA folds amenable for binding of selective small-molecule modulators and inhibitors supports the notion of RNA as an emerging drug target.[3−6] Discovery of inhibitors directed at ncRNA elements has been pursued for several viruses including the human immunodeficiency virus (HIV)[7] and hepatitis C virus (HCV).[8] HCV is a pathogenic flavivirus with a positive-sense single stranded RNA genome whose translation is regulated by an internal ribosome entry site (IRES) in the 5′ untranslated region (UTR) upstream of the open reading frame. The HCV IRES is a highly structured ncRNA element which recruits host cell ribosomes directly at the viral start codon without the requirement for most translation initiation factors.[9] We have previously discovered an RNA conformational switch in subdomain IIa of the HCV IRES, which is the target for 2-amino-benzimidazole viral translation inhibitors.[8,10] Benzimidazole scaffolds have been used by others to build inhibitors of the HIV Tat protein-TAR RNA interaction[11,12] as well as ligands that target precursor micro-RNAs[13] and RNA internal loops.[14]

The HCV IRES subdomain IIa RNA adopts an L-shaped bent structural state while an extended conformation is captured by ligand binding.[15] Crystal structure analysis of the representative inhibitor **2** bound to the IRES subdomain IIa target revealed key interactions for ligand-RNA recognition which include two hydrogen bonds formed between the 2-amino-imidazole scaffold and the Hoogsteen edge of the G110 base (Figure 1).[16] Compounds like **2** emerged from medicinal chemistry optimization of the 2-amino-benzimidazole **1** (Figure 2), which was initially discovered as a hit in a mass-spectrometry screen for small molecules interacting with the HCV IRES RNA.[10] Mechanism of action studies of 2-amino-benzimidazole translation inhibitors revealed that binding of these compounds to the HCV IRES captures the subdomain IIa RNA switch in an extended conformation which blocks viral translation initiation.[15,16]

Structure−activity relationships of analogs derived from **1** along with insight provided by the cocrystal structure of **2** bound to subdomain IIa RNA suggested that the ligand binding pocket does not tolerate substituents at positions 6 and 7, in vicinity to the hydrogen bonding face of the 2-amino-imidazole scaffold, as is evident from the inactivity of compounds like **3**.[10,16] Efforts to replace the imidazole ring by the less basic oxazole led to active compounds such as **4** and suggested that other heterocycles with appropriate hydrogen donor edges may be used to furnish ligands with more drug-like physicochemical properties for targeting subdomain IIa RNA.[17]

This notion is supported by the discovery that the subdomain IIa switch binds guanosine as a natural ligand which recognizes the RNA pocket through interactions with the guanine base.[18] While guanine (**5**) and the related 2-amino-quinazolinone **6** have only weak affinity for the RNA target, the interaction is selective and exploits the 2-amino-pyrimidinone ring as a hydrogen bond donor motif that is structurally similar to the 2-amino-imidazole scaffold but less basic. The 2-fold

Received: August 9, 2016
Accepted: October 24, 2016
Published: October 24, 2016

DOI: 10.1021/acschembio.6b00687
ACS Chem. Biol. XXXX, XXX, XXX−XXX

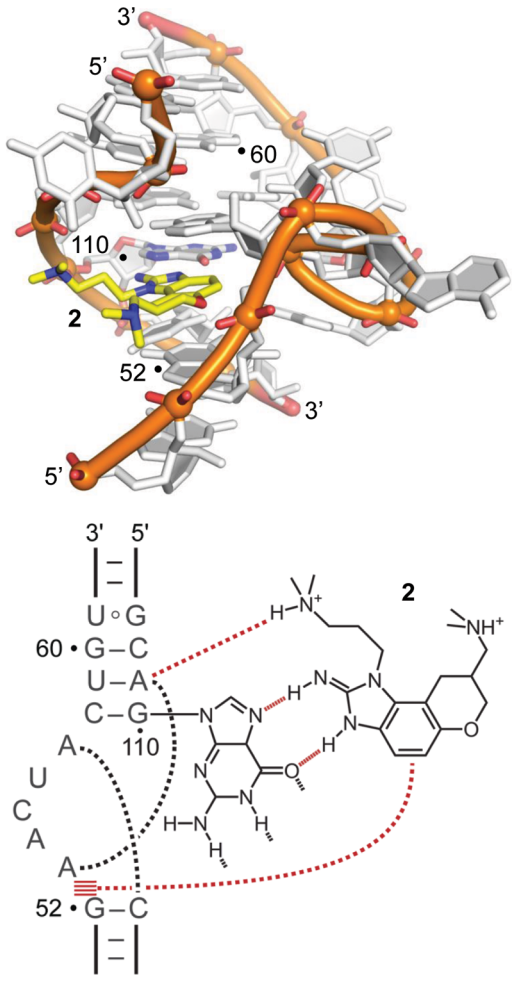

Figure 1. Crystal structure of the HCV IRES subdomain IIa RNA complex with the viral translation inhibitor **2**.[16] Key interactions of the 2-amino-benzimidazole ligand with the RNA target involve hydrogen bonding to G110 and partial intercalation between G52 and A53.

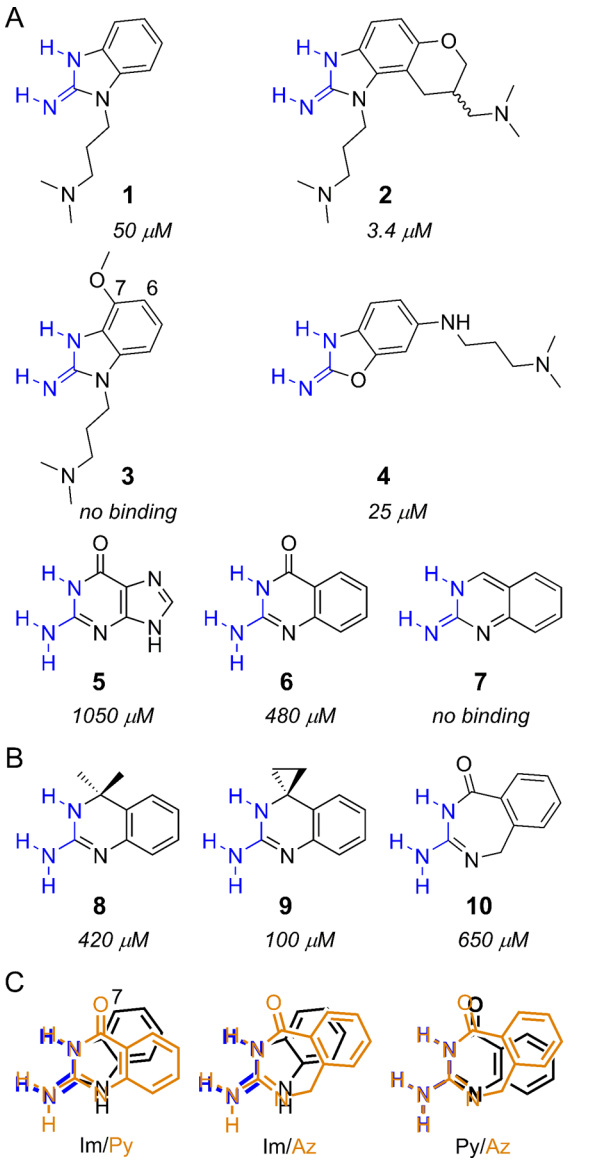

Figure 2. Ligands of the HCV IRES subdomain IIa and their binding affinity to the subdomain IIa RNA target. (A) Previously identified ligands: benzimidazole viral translation inhibitors **1** and **2**,[10,15,16] inactive benzimidazole derivative **3**,[10] benzoxazole inhibitor **4**,[17] natural ligand guanine **5**,[18] 2-amino-quinazolinone **6**,[18] and 2-amino-quinazoline **7**. (B) New ligands synthesized in this work: 2-amino-quinazoline derivatives **8** and **9** and benzodiazepinone **10**. The guanidine-like hydrogen bond donor motif highlighted in blue was identified in the cocrystal structure of **2** bound at the subdomain IIa RNA to provide key interactions for target recognition.[16] Tautomers are shown that reveal the H-bond donor motif. Binding affinity is indicated below the compound number as EC_{50} value [μM] determined in a FRET-based target binding assay.[19,20] (C) Superposition of scaffolds: Im = benzimidazole, Py = pyrimidinone in quinazolinone and guanine, and Az = diazepinone, showing corresponding hydrogen bond donor groups used for manual docking at the subdomain IIa ligand binding pocket (Figure 3).

better target affinity of **6** compared to guanine (**5**) is likely due to improved stacking interactions of RNA bases G52 and A53 with the benzene ring in **6** versus the imidazole in **5**. Manual docking of **5** and **6** to the crystal structure of the subdomain IIa RNA in complex with **2** revealed a small pocket extending at the back side of the ligand binding site, which may accommodate the carbonyl of 2-amino-pyrimidinone derivatives (guanine and quinazolinones) and the 7-methine group of the 2-amino-benzimidazoles (Figure 2, panel C) but not the larger 7-methoxy substituent of **3** (Figure 3). Occupation of the back-side pocket may support correct ligand positioning. The 2-amino-quinazoline **7** lacks a substituent at the 4-position and does not bind to the subdomain IIa RNA, which may in part be caused by the unfavorable tautomer that presents the hydrogen bond donor motif required for target recognition.

Inspection of the back-side pocket in the ligand binding site of subdomain IIa RNA suggested that a small nonplanar substituent may be accommodated and thereby confer higher binding affinity to ligands derived from the 2-amino-quinazoline scaffold. Since the composition of RNA functional groups lining the back-side pocket did not indicate directional hydrogen bonding interactions with the carbonyl group of the docked guanine (**5**) or 2-amino-quinazolinone (**6**), we considered introducing compact nonpolar substituents to improve shape complementarity of ligands at the subdomain IIa ligand binding site. To test our hypothesis, we designed compounds **8** and **9**, which carried dimethyl or spiro-cyclopropyl substitutions instead of a carbonyl group at the 2-amino-quinazoline 4-position (Figure 2, panel B). Both substitutions would extend the ligand shape out of planarity to

DOI: 10.1021/acschembio.6b00687
ACS Chem. Biol. XXXX, XXX, XXX−XXX

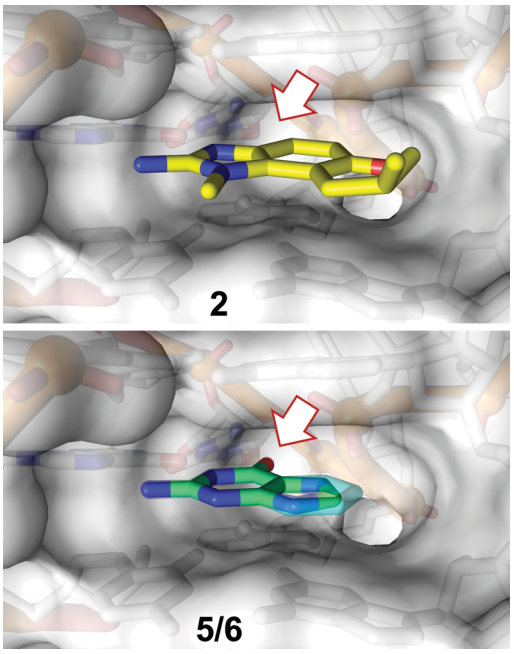

Figure 3. Ligand interaction with the HCV IRES subdomain IIa in the crystal structure of the 2-amino-benzimidazole translation inhibitor **2** bound to the RNA target (yellow)[16] and docked superimposed models of guanine **5** (green) and 2-amino-quinazolinone **6** (light blue). The arrow indicates a pocket at the back of the ligand binding site, revealed in the cocrystal structure with **2**, which may accommodate the carbonyl group of **5** and **6**, or slightly larger substituents such as the spiro-cyclopropyl moiety in compound **9**.

Scheme 1. Synthesis of 4,4-dimethyl-2-amino-3,4-dihydroquinazoline 8, 2-amino-quinazoline spiro-cyclopropyl analog 9, and 3-amino-benzodiazepinone 10

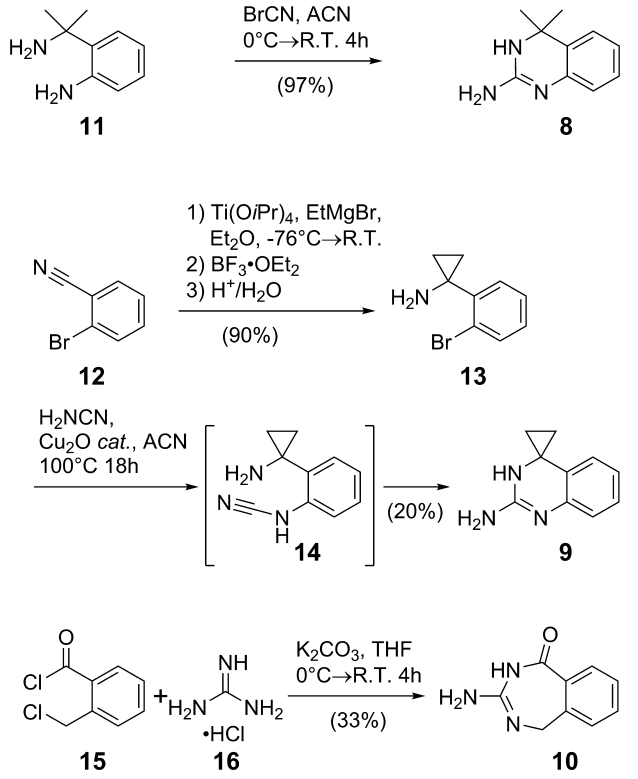

potentially achieve better shape complementarity in the back-side pocket of the RNA target. Since the spiro-cyclopropyl group provides a slightly more compact extension than the dimethyl modification, binding testing of analogs **8** and **9** in comparison to the parent scaffold **6** will provide information on the impact of subtle shape changes on ligand affinity. Prediction of drug-likeness based on established cheminformatics metrics suggested that derivatives of 2-amino-quinazoline, including **8** and **9**, are more drug-like chemotypes than 2-amino-benzimidazole analogs (Supporting Information Figure 1).

In a complementary approach of probing the impact of ligand shape on occupation of the subdomain IIa target site, we designed a 3-amino-benzodiazepinone (**10**) which had an overall increased molecular volume compared to 2-amino-quinazolinone **6** and positioned the benzene ring in an orientation that more closely resembled the 2-amino-benzimidazoles while retaining the carbonyl group directed at the back-side pocket (Figure 2, panel C).

The dimethyl derivative **8** was prepared at high yield in one step by cyclization of diamine **11** with cyanogen bromide (Scheme 1).[21] Synthesis of analog **9** commenced with the construction of the spiro-cyclopropyl ring through conversion of *o*-bromobenzonitrile **12** in the Kulinkovich–Szymoniak procedure (Scheme 1).[22] In this reaction, an ethyl Grignard reagent and titantium(IV) isopropoxide form a titanacyclopropane reagent which adds to the nitrile to furnish an intermediate that is converted to the cyclopropyl amine **13** by the addition of a Lewis acid (BF_3). To furnish the analog **9**, we attempted a one-pot reaction of the aryl bromide in **13** with cyanamide in a copper(I)-catalyzed Ullmann amination[23] followed by thermally driven intramolecular cyclization of the intermediate **14**. The 3-amino-benzodiazepinone **10** was obtained in a one-pot cyclization of the benzoyl chloride precursor **15** with guanidinium chloride (**16**) in the presence of a base (Scheme 1). The final products **8**, **9**, and **10** were purified by reverse-phase HPLC, and their identity was established by ^{1}H and ^{13}C NMR spectroscopy as well as high-resolution mass spectrometry.

Compounds **8**, **9**, and **10** were assessed in a FRET-based assay that we previously developed to monitor and quantify ligand binding to the IRES subdomain IIa.[19,20] The assay measures ligand affinity by quantifying the fraction of RNA target captured in the ligand-bound extended state, which results in FRET quenching relative to the signal from the ligand-free bent RNA. Ligand affinities for the subdomain IIa reported in Figure 2 were determined by the FRET assay in previous studies[8,15,17,18] and for compounds **8**, **9**, and **10** in the current study. The dimethyl analog **8** bound to the RNA target with an affinity comparable to 2-amino-quinazolinone **6** as indicated by an EC_{50} value of 420 ± 60 μM in dose–response FRET titrations. In contrast, the spiro-cylopropyl derivative **9** showed about 4-fold tighter binding with an EC_{50} value of 100 ± 26 μM. Among the three tested compounds, the 3-amino-benzodiazepinone **10** was the weakest binder of the subdomain IIa with an EC_{50} value of 650 ± 130 μM. The nonplanar structure of the diazepinone ring in **10** may lead to steric clash with the intercalation site between the RNA bases G52 and A53 and thereby weaken ligand affinity. In addition, ^{1}H and ^{13}C NMR spectra of **10** suggest that this compound was isolated as a difficult to separate mixture of two tautomers, among which one may lack the hydrogen bond donor motif required for target recognition (see Supporting Information).

Binding of **8** and **9** to the subdomain IIa RNA demonstrates that substitution at the quinazoline 4-position is beneficial for

DOI: 10.1021/acschembio.6b00687
ACS Chem. Biol. XXXX, XXX, XXX–XXX

target recognition. The polar carbonyl group in **6** or two hydrophobic methyl groups in **10**, both impart RNA target binding to a similar extent. The importance of precise shape complementarity between the ligand and RNA pocket is revealed by the over 4-fold better affinity of the spiro-cyclopropyl analog **9** compared to **6** and **8**. Molecular volume calculations (see Supporting Information) show that the carbonyl group of **6** adds ∼8 Å^3 at the 4-position of the quinazoline while the methyl substituents of **8** and the spiro-cyclopropyl modification of **9** add ∼38 Å^3 and ∼28 Å^3, respectively. The compact spiro-cyclopropyl substituent seems to fit the back-side pocket in the subdomain IIa ligand binding site better than the bulkier dimethyl modification. Comparable affinities of **6** and **8** along with the even tighter binding of **9** suggest that space-filling occupation of the back-side pocket in the ligand binding site dominates over polar interactions that a substituent might contribute at this position. These findings are in agreement with the observation that the composition of RNA functional groups lining the back-side pocket does not provide for directional hydrogen bond formation.

In summary, we used a structure-guided approach to design heterocyclic compounds that target the viral translation inhibitor binding site in the HCV IRES subdomain IIa to explore optimization of ligand shape complementarity while improving drug-likeness. The goal was to discover alternative scaffolds suitable for future efforts of replacing the 2-amino-benzimidazole core of previously described viral, translation inhibitors. While none of the newly synthesized scaffolds (**8**, **9**, **10**) showed a binding affinity that warranted testing of the compounds in an *in vitro* functional or cell-based assay, we demonstrated that the basic 2-amino-imidazole scaffold of previously discovered translation inhibitors can be replaced with a 2-amino-quinazoline heterocycle to obtain ligands with more drug-like physicochemical properties. Modification of a 2-amino-quinazoline derivative with a compact nonplanar spiro-cyclopropyl substituent that targets a small pocket at the back side of the inhibitor binding site led to affinity improvement of the resulting ligand **9** to a level that was comparable to the 2-amino-benzimidazole core scaffold. The observation that a spiro-cyclopropyl modification increased ligand binding at the subdomain IIa target suggests that careful placement of nonpolar groups that improve shape complementarity provides a useful strategy for optimization of compounds binding RNA despite the hydrophilic nature of the target. Future efforts of HCV translation inhibitor synthesis will explore substituted analogs derived from the 2-amino-quinazoline derivative **9** as a shape-optimized scaffold for targeting the viral IRES RNA target.

METHODS

Synthesis and Characterization of Compounds. See the Supporting Information.

FRET Assay. Compounds were tested for binding to the HCV IRES subdomain IIa in a FRET assay and EC_{50} values of binding calculated from triplicate dose−response titrations as previously described.[19,20]

ASSOCIATED CONTENT

Supporting Information

The Supporting Information is available free of charge on the ACS Publications website at DOI: 10.1021/acschembio.6b00687.

Synthetic procedures and compound characterization (PDF)

AUTHOR INFORMATION

Corresponding Author

*Tel.: +1 858 534 4467. E-mail: tch@ucsd.edu.

Present Address

§Norac Pharma, Inc., Azusa, CA 91702, United States

Author Contributions

B.P.C. and M.A.B. performed experiments. T.H. designed compounds and wrote the manuscript. All authors analyzed data and have given approval to the final version of the manuscript.

Funding

The research was supported in part by the UCSD Academic Senate. M.A.B. was supported by a GAANN fellowship from the U.S. Department of Education. Instrumentation at the UCSD Biomolecule Crystallography Facility was acquired with funding from the National Institutes of Health, grant OD011957. The NMR facility was supported by the National Science Foundation, CRIF grant CHE-0741968.

Notes

The authors declare no competing financial interest.

ACKNOWLEDGMENTS

We are grateful to E. Romero for helpful discussions and suggestions.

REFERENCES

(1) Hermann, T. (2016) Small molecules targeting viral RNA. *Wiley Interdiscip. Rev. RNA 7*, 726−743.

(2) Morris, K. V., and Mattick, J. S. (2014) The rise of regulatory RNA. *Nat. Rev. Genet. 15*, 423−437.

(3) Hermann, T. (2000) Strategies for the design of drugs targeting RNA and RNA-protein complexes. *Angew. Chem., Int. Ed. 39*, 1890−1904.

(4) Gallego, J., and Varani, G. (2001) Targeting Rna with small-molecule drugs: therapeutic promise and chemical challenges. *Acc. Chem. Res. 34*, 836−843.

(5) Thomas, J. R., and Hergenrother, P. J. (2008) Targeting RNA with small molecules. *Chem. Rev. 108*, 1171−1224.

(6) Guan, L., and Disney, M. D. (2012) Recent advances in developing small molecules targeting RNA. *ACS Chem. Biol. 7*, 73−86.

(7) Le Grice, S. F. (2015) Targeting the HIV RNA genome: high-hanging fruit only needs a longer ladder. *Curr. Top. Microbiol. Immunol. 389*, 147−169.

(8) Dibrov, S. M., Parsons, J., Carnevali, M., Zhou, S., Rynearson, K. D., Ding, K., Garcia Sega, E., Brunn, N. D., Boerneke, M. A., Castaldi, M. P., and Hermann, T. (2014) Hepatitis C virus translation inhibitors targeting the internal ribosomal entry site. *J. Med. Chem. 57*, 1694−1707.

(9) Ji, H., Fraser, C. S., Yu, Y., Leary, J., and Doudna, J. A. (2004) Coordinated assembly of human translation initiation complexes by the hepatitis C virus internal ribosome entry site RNA. *Proc. Natl. Acad. Sci. U. S. A. 101*, 16990−16995.

(10) Seth, P. P., Miyaji, A., Jefferson, E. A., Sannes-Lowery, K. A., Osgood, S. A., Propp, S. S., Ranken, R., Massire, C., Sampath, R., Ecker, D. J., Swayze, E. E., and Griffey, R. H. (2005) SAR by MS: discovery of a new class of RNA-binding small molecules for the hepatitis C virus: internal ribosome entry site IIA subdomain. *J. Med. Chem. 48*, 7099−7102.

(11) Ranjan, N., Kumar, S., Watkins, D., Wang, D., Appella, D. H., and Arya, D. P. (2013) Recognition of HIV-TAR RNA using neomycin-benzimidazole conjugates. *Bioorg. Med. Chem. Lett. 23*, 5689−5693.

DOI: 10.1021/acschembio.6b00687
ACS Chem. Biol. XXXX, XXX, XXX−XXX

(12) Kumar, S., Ranjan, N., Kellish, P., Gong, C., Watkins, D., and Arya, D. P. (2016) Multivalency in the recognition and antagonism of a HIV TAR RNA-TAT assembly using an aminoglycoside benzimidazole scaffold. *Org. Biomol. Chem. 14*, 2052−2056.
(13) Velagapudi, S. P., Gallo, S. M., and Disney, M. D. (2014) Sequence-based design of bioactive small molecules that target precursor microRNAs. *Nat. Chem. Biol. 10*, 291−297.
(14) Velagapudi, S. P., Pushechnikov, A., Labuda, L. P., French, J. M., and Disney, M. D. (2012) Probing a 2-aminobenzimidazole library for binding to RNA internal loops via two-dimensional combinatorial screening. *ACS Chem. Biol. 7*, 1902−1909.
(15) Parsons, J., Castaldi, M. P., Dutta, S., Dibrov, S. M., Wyles, D. L., and Hermann, T. (2009) Conformational inhibition of the hepatitis C virus internal ribosome entry site RNA. *Nat. Chem. Biol. 5*, 823−825.
(16) Dibrov, S. M., Ding, K., Brunn, N. D., Parker, M. A., Bergdahl, B. M., Wyles, D. L., and Hermann, T. (2012) Structure of a hepatitis C virus RNA domain in complex with a translation inhibitor reveals a binding mode reminiscent of riboswitches. *Proc. Natl. Acad. Sci. U. S. A. 109*, 5223−5228.
(17) Rynearson, K. D., Charrette, B., Gabriel, C., Moreno, J., Boerneke, M. A., Dibrov, S. M., and Hermann, T. (2014) 2-Aminobenzoxazole ligands of the hepatitis C virus internal ribosome entry site. *Bioorg. Med. Chem. Lett. 24*, 3521−3525.
(18) Boerneke, M. A., Dibrov, S. M., Gu, J., Wyles, D. L., and Hermann, T. (2014) Functional conservation despite structural divergence in ligand-responsive RNA switches. *Proc. Natl. Acad. Sci. U. S. A. 111*, 15952−15957.
(19) Zhou, S., Rynearson, K. D., Ding, K., Brunn, N. D., and Hermann, T. (2013) Screening for inhibitors of the hepatitis C virus internal ribosome entry site RNA. *Bioorg. Med. Chem. 21*, 6139−6144.
(20) Boerneke, M. A., and Hermann, T. (2015) Conformational flexibility of viral RNA switches studied by FRET. *Methods 91*, 35−39.
(21) Ishikawa, F., Watanabe, Y., and Saegusa, J. (1980) Cyclic guanidines. IX. Synthesis of 2-amino-3,4-dihydroquinazolines as blood platelet aggregation inhibitors. *Chem. Pharm. Bull. 28*, 1357−1364.
(22) Bertus, P., and Szymoniak, J. (2003) A direct synthesis of 1-aryl- and 1-alkenylcyclopropylamines from aryl and alkenyl nitriles. *J. Org. Chem. 68*, 7133−7136.
(23) Jiao, J., Zhang, X. R., Chang, N. H., Wang, J., Wei, J. F., Shi, X. Y., and Chen, Z. G. (2011) A facile and practical copper powder-catalyzed, organic solvent- and ligand-free Ullmann amination of aryl halides. *J. Org. Chem. 76*, 1180−1183.

DOI: 10.1021/acschembio.6b00687
ACS Chem. Biol. XXXX, XXX, XXX−XXX